Supplementary material: [Appendix, numericla benchmark] is available at www.geolsoc.org.uk/SUP00000

The models presented in this paper use the finite-differences code Parovoz (Poliakov & Podladchikov, 1992; Podladchikov et al., 1993), which is based on the FLAC method (Cundall & Board, 1988), and builts a quadrilateral Lagrangian mesh. This condition requires to incorporate the chamber inside the mesh if one wishes to achieve a very high mesh resolution. Then, the elastic properties of the meshed chamber determine its capacity to dilate, and thus the amount of pressure transfered through its walls into the bedrock domain. Consequently, internal overpressure is best measured by the maximum deviatoric stress recorded at the modeled magmatic chamber walls (e.g. Chery et al., 1991), and is the value to compare with analytical predictions. Differences in modeled results are thus expected when compared to models with « empty chambers » meshes.

Here we benchmark our models with a finite element code, ADELI (Hassani et al., 1997; Chery et al., 2001), with triangular mesh elements and an explicit dynamic relaxation method similar to FLAC, The mesh can be defined radial about the chambers' circular boundary. Adeli has been widely applied to various geodynamical settings (e.g. http://www.dstu.univ-montp2.fr/PERSO/chery/Adeli_web/doc/publis2007.htm), and the method details can be found for example in Chery et al. (2001). Because of computational time issues, mesh resolution in Adeli is chosen of the order of 50 m at the chambers' wall, 2 times coarser than in Parovoz.

Plasticity in Adeli is accounted for slightly differently than in Parovoz. At failure, Parovoz employs the Mohr-Coulomb failure criterion by means of an explicit algorithm, whereas Adeli employs an implicit algorithm and the Drucker-Praeger yield criterion. Therefore, despite friction angle and cohesion being defined in Adeli to coincide with conventional Mohr-Coulomb values, slight differences still remain, In addition, Adeli does not include a tensile cutoff strength, but instead the default tensile strength deduced from cohesion $T_o = S_o/\tan\varphi$. Therefore this value is also taken in Parovoz for the present benchmarks.

A1) Benchmark under mostly elastic conditions, ΔP=50MPa

Stress and strain at the surface obtained in our reference model (Fig. 4) are compared with those obtained with Adeli, at the specific internal overpressure ΔP=50MPa. At this stage, most of the domain is elastic, apart from a few hundred meters below the ground surface at origin Xo. 4 models are displayed, with purely elastic and elasto-plastic solutions for each code Parovoz and Adeli.

Fig. A1 from top to bottom, displays surface displacements and horizontal stress at the surface (top figures), and 2D contours of failure zones, shear-strain and shear-stress for Parovoz and for Adeli, in the middle and bottom of the figure, respectively.

Elastic solutions are nearly undistinguishable from elasto-plastic solutions for each code, except for the horizontal stress (σ_{xx}) at the origin where failure has initiated: in this case σ_{xx} is limited by the rock tensile strength in Parovoz, whereas Adeli's failure criterion allows for a higher yield at the same location. Also, differences in mesh resolution lead to different averaged stress over an element thickness, therefore also, the occurrence of local differences. This explains why rock failure at the top surface has a slightly greater extent in Parovoz than in Adeli.

In general, modeled surface displacements are greater in Adeli than in Parovoz by about 5% (maximum uplift of 2.13 m versus 2.05 m, Table 1). We attribute this difference to the combined effect of the emptyness of the chamber in Adeli, and local numerical discontinuities at the stair-shape wall geometry of the chamber in Parovoz, which increase the shear strain there.

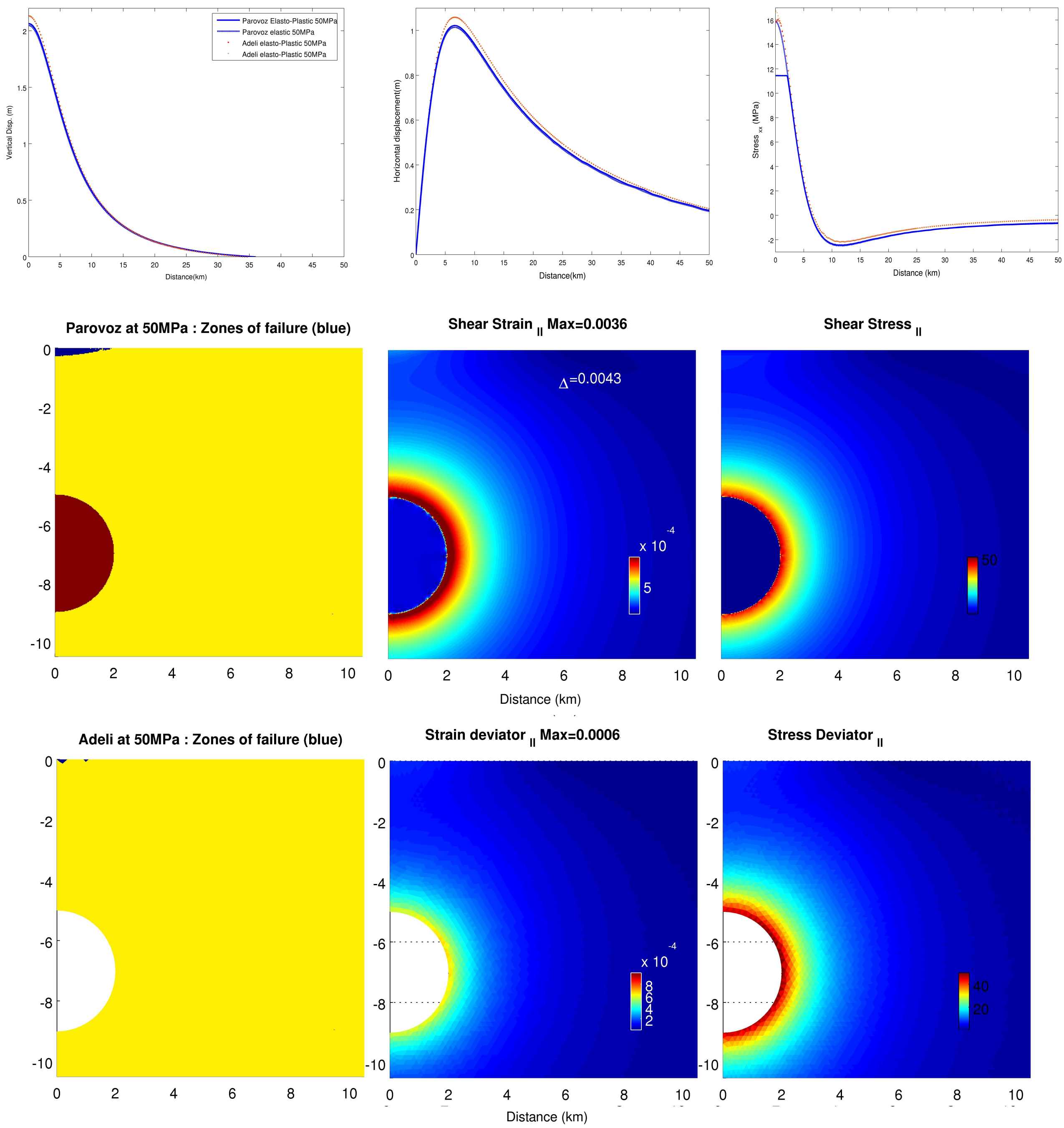

Fig. A1.

A2) Benchmarks for a mostly plastic domain, ΔP=120MPa

Now we compare results between Parovoz and Adeli for an internal overpressure of ΔP=120MPA, so that the domain in between the chamber and the ground surface is in majority at a state of plastic yield. In this case, the chamber's wall mesh elements are progressively submitted to a stress level much above their yield stress, therefore numerical artifacts are expected to be favored here.

We observe in Fig. A2.(top) that modeled surface displacements and stress with Parovoz are generally smaller than those obtained with Adeli, again by about 5% (e.g. Table 1). The failure domain in Parovoz has a greater extent than in Adeli at ΔP=120 MPa. However, very good consistency is seen in between the Parovoz model at ΔP=120 MPa and the Adeli model at ΔP=150 Mpa (Figure A2, bottom). From additional models with frictionless material (not shown here), we believe that these differences are partly related to the different algorithmic procedures for plastic yielding employed in Parovoz and Adeli (explicit Mohr-Coulomb versus implicit Drucker-Praeger in Adeli).

A3) Benchmarks without gravity ΔP= 15 and 18 MPa

Models without gravity (equivalent to a state of lithostatic pore fluid pressure) are also compared with Parovoz and Adeli. For ΔP =15 MPa, surface displacements and horizontal stress are in extremely good agreement (Fig. A3, top). However, the failure pattern occurs over a circular domain around the chamber significantly thinner with Adeli than with Parovoz (middle figures in Fig. A3). We also plotted failure patterns which look very similar, and correspond to ΔP=18.1 MPa in Parovoz and ΔP =18.9 MPa in Adeli (bottom lines in Fig. A3). Note, as in Fig. A2, the peculiar ear shape of the plastified domain, which is similar to that obtained in other studies (e.g. Massinas & Sakellariou, 2009, Fig. 2d, or Chery et al., 1991).

In conclusion, this benchmark shows a relatively good consistency of the model results obtained with Parovoz and with Adeli, considering that differences obviously rise from different mesh resolutions, mesh geometries (meshed versus unmeshed chamber), and numerical handling of constitutive laws. In order to obtain a better mechanical solution relieved from numerical artefacts, additional comparisons with other numerical tools throughout the community would be necessary. A collective project such as that developed to compare the geometry of faults in thrust nappes (Buiter et al., 2008) would be recommended. This latter benchmark showed that whereas results are qualitatively similar, it remains difficult to match shear band geometries exactly, since the highly non-linear process of failure depends on specific formulations used in each numerical method (e.g .Kaus, 2010; Yarushina et al., 2010).

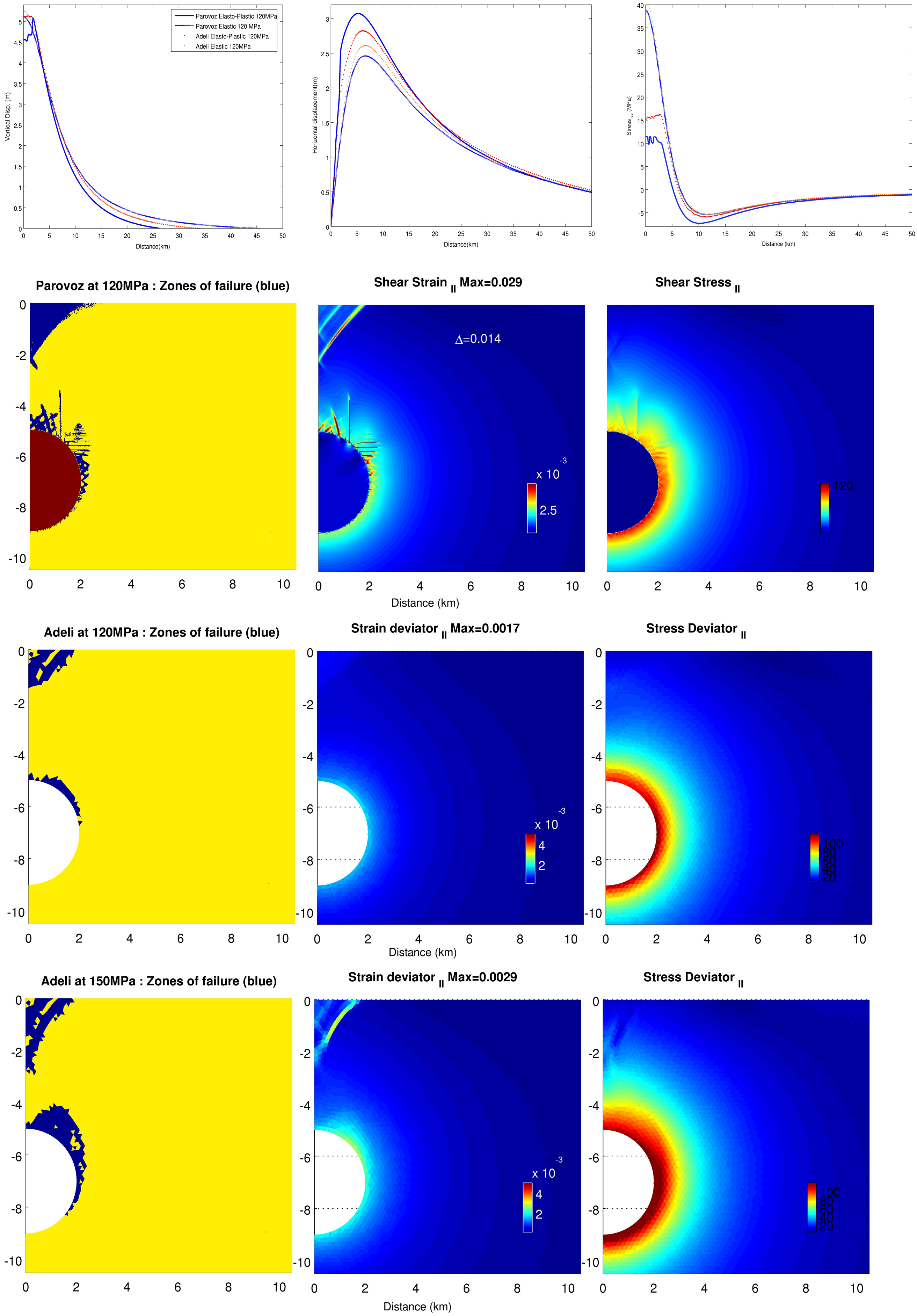

Parovoz Elasto-Plastic 120MPa
Parovoz Elastic 120 MPa
Adeli Elasto-Plastic 120MPa
Adeli Elastic 120MPa
Vertical Disp. (m)
Distance(km)
Horizontal displacement(m)
Distance(km)
Stress xx (MPa)
Distance (km)
Parovoz at 120MPa : Zones of failure (blue)
Shear Strain II Max=0.029
Shear Stress II
Δ=0.014
x 10 -3
2.5
120
Distance (km)
Adeli at 120MPa : Zones of failure (blue)
Strain deviator II Max=0.0017
Stress Deviator II
x 10 -3
4
2
Distance (km)
Adeli at 150MPa : Zones of failure (blue)
Strain deviator II Max=0.0029
Stress Deviator II
x 10 -3
4
2
Distance (km)

Fig. A2

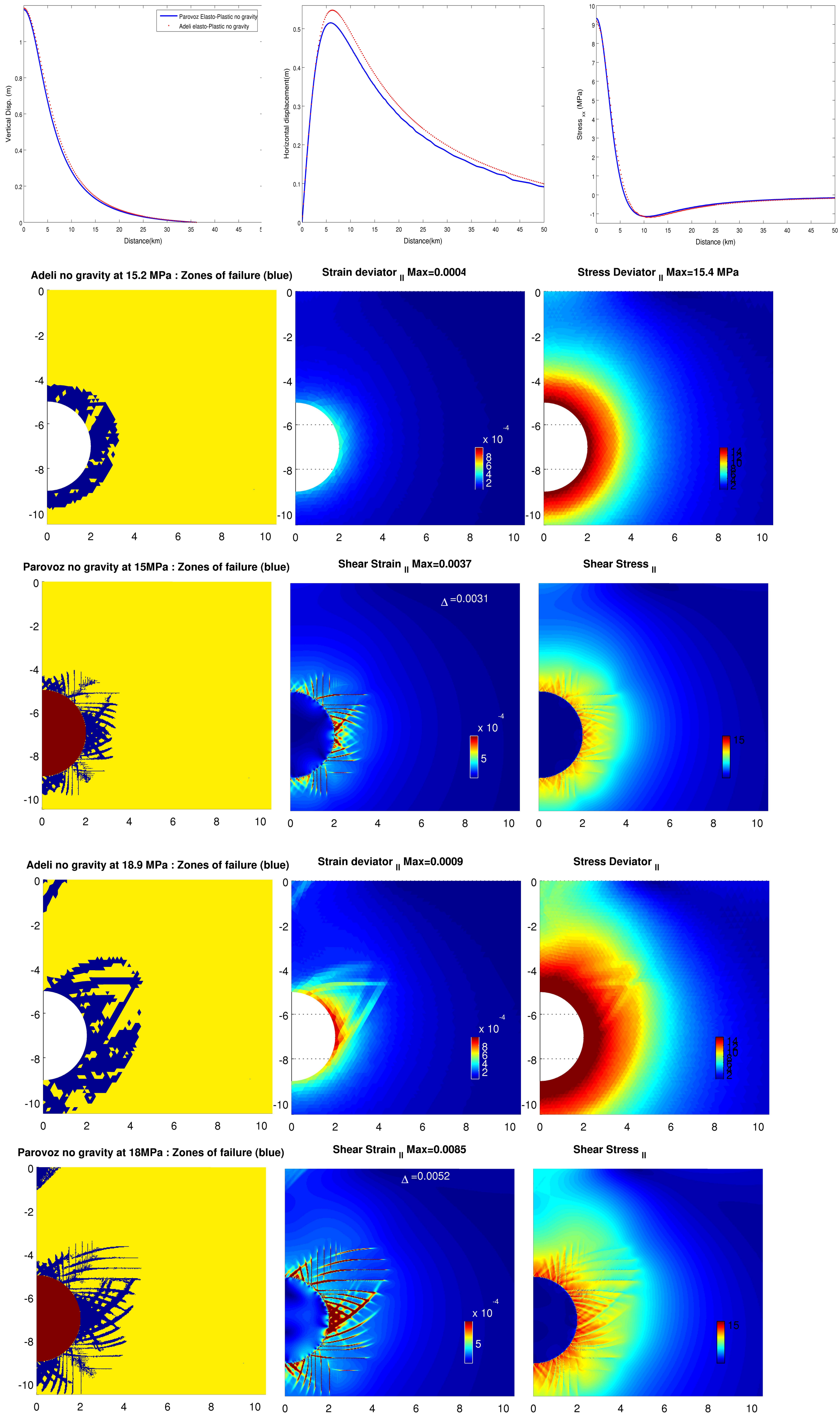

Parovoz Elasto-Plastic no gravity
Adeli elasto-Plastic no gravity
Vertical Disp. (m)
Distance(km)
Horizontal displacement(m)
Distance(km)
Stress xx (MPa)
Distance (km)
Adeli no gravity at 15.2 MPa : Zones of failure (blue)
Strain deviator II Max=0.0004
Stress Deviator II Max=15.4 MPa
Parovoz no gravity at 15MPa : Zones of failure (blue)
Shear Strain II Max=0.0037
Δ=0.0031
Shear Stress II
Adeli no gravity at 18.9 MPa : Zones of failure (blue)
Strain deviator II Max=0.0009
Stress Deviator II
Parovoz no gravity at 18MPa : Zones of failure (blue)
Shear Strain II Max=0.0085
Δ=0.0052
Shear Stress II

Fig. A3.